Energy Proceedings
Vol 53, 2025
ISSN 2004-2965

Numerical Analysis on Desorption Process of K_2CO_3 for Thermochemical Heat Storage[#]

Sitong Li[1], Zhuqing Li[1], Yu Chen[1], Hua Tian[1*], Gequn Shu[1,2]

1 State Key Laboratory of Engines, Tianjin University, No.92 Weijin Road, Nankai District, Tianjin 300072, the People's Republic of China

2 Department of Thermal Science and Energy Engineering, University of Science and Technology of China, No.96 Jinzhai Road, Baohe District, Hefei 230027, the People's Republic of China
(Corresponding Author: thtju@tju.edu.cn)

ABSTRACT

Energy storage technology can significantly enhance energy efficiency and conserve energy. Thermochemical adsorption heat storage based on salt hydrate is a crucial technology for long-term energy storage owing to its significant advantages of excellent energy storage density and minimal heat loss. K_2CO_3 is regarded as a prospective thermochemical heat storage material. In this work, a numerical model of the K_2CO_3 heat storage process is established using COMSOL based on the conservation of mass, momentum and energy, considering the variation of porosity with conversion degree and the flow of water vapor. Literature results confirm the validity of this model. The heat storage process is investigated, and the transient evolution of parameters such as temperature and concentration during the desorption process is described, elucidating the fundamental principles of the thermochemical heat storage process. The influence of various parameters on system performance is explored. The simulation results show that the porosity of the heat storage material shows obvious inhomogeneity in time and space. The porosity increases continuously with the progress of the reaction, which effectively promotes the progress of the reaction. Raising the heat flux and reducing heat loss can effectively decrease the reaction start-up time. This work offers insights into designing and optimizing thermochemical heat storage material and system.

Keywords: salt hydrate, K_2CO_3, thermochemical energy storage, numerical analysis, variable porosity

NONMENCLATURE

Abbreviations	
EG	Expanded Graphite
EVM	Expanded Vermiculite
TCES	Thermochemical Energy Storage
TES	Thermal Energy Storage
Symbols	
A	Frequency factor
c	Concentration
c_p	Heat capacity
d_p	Salt particle diameter
E	Activation energy
H	Reaction enthalpy
k	Thermal conductivity
M	Molar mass
p	Pressure
Q	Heat source
R	Universal gas constant
r	Reaction rate constant
T	Temperature
Greek Letters	
α	Conversion degree
ε	Porosity
ρ	Density
κ	Permeability
μ	Viscosity
Subscripts	
h	Salt hydrate
s	Anhydrous salt
g	Water vapor
0	Initial

1. INTRODUCTION

As the global energy crisis intensifies, renewable energy becomes a key solution [1]. Thermal energy storage (TES) technology balances energy supply and demand and facilitates energy utilization [2]. TES technologies are categorized into sensible, latent and

This is a paper for the 16th International Conference on Applied Energy (ICAE2024), Sep. 1-5, 2024, Niigata, Japan.

thermochemical energy storage (TCES) [3]. TCES is regarded as a promising heat storage technology because of its high energy storage density and almost no heat loss [4]. Among them, salt hydrate-based thermochemical adsorption heat storage provides the benefits of simple operation and exceptional reliability, and is widely utilized in the field of medium and low-temperature heat storage [5].

K_2CO_3 is considered to be an attractive thermochemical heat storage material owing to its simple reaction, economical price and favorable stability [6]. The thermochemical adsorption heat storage based on K_2CO_3 can be expressed as:

$$K_2CO_3 \cdot 1.5\ H_2O_{(s)} + \Delta H \underset{\text{discharging}}{\overset{\text{charing}}{\rightleftharpoons}} K_2CO_{3(s)} + 1.5\ H_2O_{(g)}$$

In the heat storage process, the salt hydrate $K_2CO_3 \cdot 1.5H_2O$ absorbs heat and decomposes into anhydrous salt K_2CO_3 and water vapor. In the heat release process, the anhydrous salt and vapor react to form the salt hydrate and release heat.

Currently, K_2CO_3 is widely investigated [7, 8]. To further enhance the TES performance of the material and ameliorate the phenomena such as deliquescence and agglomeration, composites such as K_2CO_3/Expanded vermiculite (EVM) and K_2CO_3/ Expanded graphite (EG) have been developed [9, 10]. Numerical simulation is an important means to establish correct and effective theoretical model. Kant et al. [11] established a three-dimensional numerical model of the heat release process of K_2CO_3 in a honeycomb heat exchanger and pointed out that the reaction rate and heat transfer performance depend largely on the geometric parameters of the heat exchanger. Mahmoudi et al. [8] developed a CFD-DEM model to study heat and mass transfer at the particle and bed scale in a closed system. Luo et al. [6] established a three-dimensional numerical model of a serpentine tube reactor to simulate the heat release process of K_2CO_3. The results show that higher thermal fluid inlet flow rate corresponds to better heat transfer performance.

In the current study, the porosity of the heat storage material is assumed to be uniform and constant. However, in practice, the porosity varies with the degree of reaction. The flow of vapor is also an important factor to be considered in the heat storage process. TCES process is not well described in the literature. To further reflect the real thermochemical heat storage process, a two-dimensional model of TCES based on K_2CO_3 is constructed in this paper. Considering the change of porosity with conversion degree and the flow of water vapor, the TCES process is studied. The transient evolution of parameters such as temperature and concentration during the desorption process is described, revealing the basic principles of the TCES process. The effects of different parameters (heat flux and heat loss) on system performance are explored.

2. MODEL CONSTRUCTION

2.1 Mathematical model

A two-dimensional closed region with dimensions of 0.01 m × 0.01 m filled with heat storage material salt hydrate $K_2CO_3 \cdot 1.5H_2O$ is considered. The upper side experiences a heat flux of q = 1000 W/m^2. For the other side, different insulation levels are considered by accounting for different heat losses. Points 1, 2 and 3 are located on the central axis, with coordinates of (0.005 m,0.01 m) (0.005 m,0.005 m) (0.005 m,0 m).

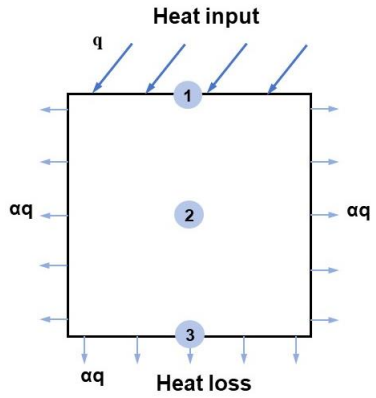

Fig. 1 Schematic diagram of the computational domain

For TCES based on salt hydrate, the hydration/ dehydration process involves “three transmissions and one reaction”. The "three transmissions" refer to mass, momentum and heat transfer, and the "one reaction" refers to the gas-solid reaction, which are coupled with each other, and are described by the mass, momentum, energy conservation equation and chemical reaction kinetics equation, respectively. Salt hydrates are considered to be porous materials and therefore the entire two-dimensional domain has an initial porosity.

2.1.1 Chemical reaction kinetics

The salt hydrate reaction rate equation can be expressed as [12]:

$$\frac{\partial c_h}{\partial t} = -rf(c_h) \quad (1)$$

where c_h is the concentration of salt hydrate and r is the chemical reaction rate constant. The desorption reaction of $K_2CO_3 \cdot 1.5H_2O$ is a first-order reaction and follows the first-order kinetic model:

$$f(c_h) = c_h \quad (2)$$

$$r = Ae^{-(E/RT)} \quad (3)$$

where A is the frequency factor, and E is the reaction activation energy.

The generation rate of anhydrous salt and the desorption rate of salt hydrate are equal, therefore:

$$\frac{\partial c_s}{\partial t} = -\frac{\partial c_h}{\partial t} \tag{4}$$

where c_s is the concentration of the anhydrous salt.

2.1.2 Mass conservation equation

The conservation of mass during thermochemical heat storage can be expressed as:

$$\frac{\partial c_i}{\partial t} + \boldsymbol{u} \cdot \nabla c_i = 0 \tag{5}$$

2.1.3 Momentum conservation equation

Darcy's law is applied to characterize the flow of water vapor in porous domains:

$$\boldsymbol{u} = -\frac{\kappa}{\mu}\nabla p \tag{6}$$

where κ is the permeability and μ is the viscosity of water vapor.

The Carman-Kozeny equation was utilized to describe the relationship between permeability and porosity:

$$\kappa = \frac{d_p^2 \varepsilon^3}{180(1-\varepsilon^3)} \tag{7}$$

where d_p is the diameter of salts and ε is the porosity in the porous domain.

2.1.4 Energy conservation equation

The energy conservation in the TCES process can be stated as follows:

$$\frac{\partial(\rho c_p T)}{\partial t} + \nabla \cdot (\rho c_p \vec{u} T) = \nabla \cdot (k \nabla T) + Q \tag{8}$$

where Q is the heat source term:

$$Q = r M_h c_h \Delta H \tag{9}$$

where M_h is the molar mass of the salt hydrate and ΔH is the dehydration enthalpy of the chemical reaction.

2.1.5 Thermophysical parameters

For heat storage material in the porous domain, the specific heat, viscosity, density and thermal conductivity vary with the porosity. To reflect more realistically the changes in the properties of salt hydrate during the desorption process, thermophysical parameters are given.

The effective density in the porous medium is denoted as:

$$\rho = (1-\varepsilon)\rho_{solid} + \varepsilon \rho_g \tag{10}$$

where ρ_{solid} is the effective density of solid salt hydrate $K_2CO_3 \cdot 1.5H_2O$ and anhydrous salt K_2CO_3, ρ_g is the density of vapor, and ε is the porosity in the porous domain. ρ_{solid} can be expressed as:

$$\rho_{solid} = \alpha \rho_{K2CO3} + (1-\alpha)\rho_{K2CO3 \cdot 1.5H2O} \tag{11}$$

where α is the conversion degree of the chemical reaction, expressed as:

$$\alpha = \frac{c_h - c_{h0}}{c_{h0}} \tag{12}$$

where c_{h0} is the initial concentration of the salt hydrate $K_2CO_3 \cdot 1.5H_2O$.

The effective heat capacity in the porous medium is as follows:

$$\rho c_p = (1-\varepsilon)(\rho c_p)_{solid} + \varepsilon (\rho c_p)_g \tag{13}$$

where $c_{p,solid}$ is the effective specific heat capacity of the salt hydrate $K_2CO_3 \cdot 1.5H_2O$ and anhydrous salt K_2CO_3, which can be denoted as:

$$c_{p,solid} = \alpha c_{p,K2CO3} + (1-\alpha) c_{p,K2CO3 \cdot 1.5H_2O} \tag{14}$$

The effective thermal conductivity in the porous material can be expressed as:

$$\kappa = (1-\varepsilon)\kappa_{solid} + \varepsilon \kappa_g \tag{15}$$

where κ_{solid} is the effective thermal conductivity of the salt hydrate $K_2CO_3 \cdot 1.5H_2O$ and anhydrous salt K_2CO_3, which can be expressed as:

$$\kappa_{solid} = \alpha \kappa_{K2CO3} + (1-\alpha)\kappa_{K2CO3 \cdot 1.5H_2O} \tag{16}$$

The effective viscosity of water vapor in the porous domain is expressed as:

$$\mu = \frac{\mu_g}{(1-\varepsilon)^{2.5}} \tag{17}$$

where μ_g is the viscosity of vapor.

2.1.6 Variable porosity equation

In the closed two-dimensional domain, the solid composition within the porous domain changes as the reaction proceeds, which consequently affects the porosity. Changes in porosity will affect the flow of vapor in the domain, and thus affect changes in substance concentration and temperature. In practical situations, it is of great significance to consider the effect of porosity changes on heat storage process.

The porosity within the porous domain can be expressed as:

$$\varepsilon = 1 - \frac{(1-\varepsilon_0)\left(1-\alpha\frac{M_{H_2O}}{M_{K2CO3 \cdot 1.5H2O}}\right)}{\alpha\left(\frac{\rho_{K2CO3}}{\rho_{K2CO3 \cdot 1.5H2O}} - 1\right) + 1} \tag{18}$$

where ε_0 is the initial porosity within the porous domain.

2.2 Model parameters

The parameters in the model are presented in Table 1. The domain is closed and there is no mass exchange with the outside environment. The water vapor velocity is set to no-slip on all boundaries. The water vapor is considered to be incompressible. At the initial moment, c_{h0}=4000 mol/m^3, c_{s0}=c_{g0}=0 mol/m^3, T_0=303.15 K.

Table 1. Material properties of $K_2CO_3 \cdot 1.5H_2O$ [6, 13].

Parameters	Value	Description
M_h	165 g/mol	Molecular mass of $K_2CO_3 \cdot 1.5H_2O$
M_s	138 g/mol	Molecular mass of K_2CO_3
M_g	18 g/mol	Molecular mass of H_2O
ρ_h	2180 kg/m^3	Density of $K_2CO_3 \cdot 1.5H_2O$
ρ_s	2330 kg/m^3	Density of K_2CO_3
ρ_g	0.46645 kg/m^3	Density of H_2O
$c_{p,h}$	1072 J/kg/K	Specific heat of $K_2CO_3 \cdot 1.5H_2O$
$c_{p,s}$	826 J/kg/K	Specific heat of K_2CO_3
$c_{p,g}$	1975 J/kg/K	Specific heat of H_2O
k_h	1 W/m/K	Thermal conductivity of $K_2CO_3 \cdot 1.5H_2O$
k_s	0.44 W/m/K	Thermal conductivity of K_2CO_3
k_g	0.026 W/m/K	Thermal conductivity of H_2O
ΔH	64.01 kJ/mol	Dehydration enthalpy
A	1.5×10^9 1/s	Frequency factor
E	78.3 kJ/mol	Activation energy
R	8.314 J/K/mol	Universal gas constant
μ	8.9×10^{-4} pa·s	Viscosity of water vapor
T_r	343.15 K	Reaction temperature
d_p	0.5 mm	Diameter of salt particle
ε_0	0.4	Initial porosity

3. NUMERICAL IMPLEMENTATION AND MODEL VALIDATION

3.1 Numerical implementation

Thermochemical energy storage process involves complex heat/mass transfer and chemical reactions. COMSOL Multiphysics based on the finite element method is particularly suitable for solving multi-physics field models. Unstructured mesh is selected for meshing. The grid independence of the model is verified by using the transient evolution of temperature at point 1 in Fig. 1 to confirm the optimal number of grids for solution. Coarse (268), regular (638), fine (994) and relatively fine (1928) grids were used for testing, and the results are shown in Fig. 2. The fine grid can not only ensure higher calculation accuracy but also save computational time, so the fine grid is selected for calculation.

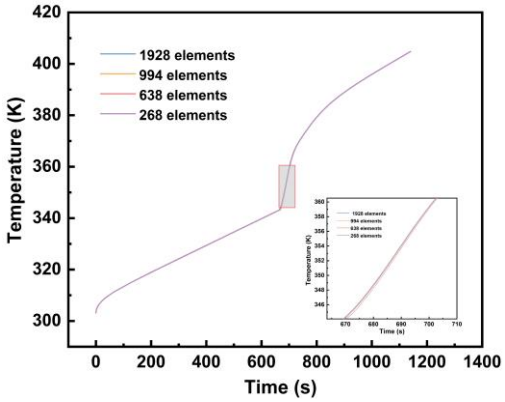

Fig. 2 Grid independence verification

3.2 Model Validation

For model validation, calculations were carried out under the same conditions as in the Ref. [14]. The temperature at point 1 was compared with the literature results. The results indicate that the calculations align well with the literature.

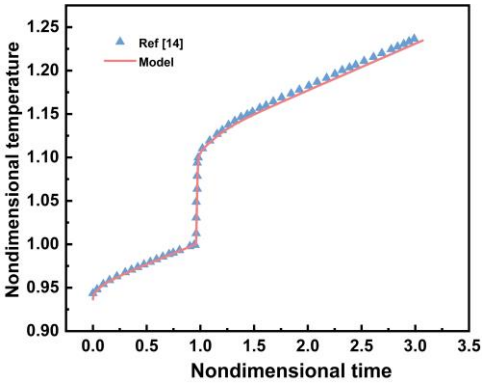

Fig. 3 Model verification

4. RESULTS AND DISCUSSION

4.1 Heat storage performance

4.1.1 Temperature evolution

The evolution of temperature with time is depicted in Fig. 4. In the first stage, heat transfer between the materials takes place through heat conduction, and the temperature increases. As temperature increases, the material reaches the chemical reaction temperature and the salt hydrate undergoes the desorption reaction, causing a sharp rise in temperature. In the third stage, as the chemical reaction ends, heat transfer continues between the materials and the temperature continues to rise. A sudden increase in temperature away from the upper boundary is observed to occur at temperatures below the chemical reaction temperature, attributed to

rapid thermal diffusion from the upper high temperature. Point 3 shows a sudden increase in temperature different from points 1 and 2, attributed to rapid heat diffusion in the upper part and chemical reactions in the lower part.

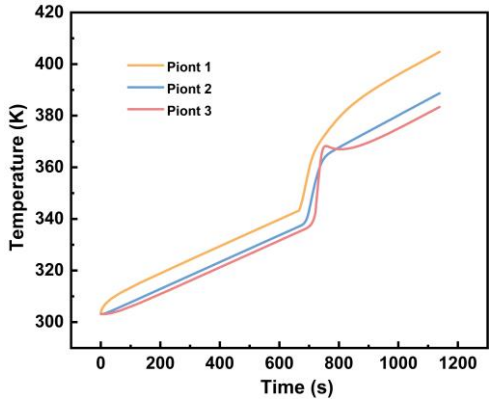

Fig. 4 Temperature evolution with time

Fig. 5 displays the temperature evolution during TCES process. Since the heat source is above, the upper material is heated first, and the temperature distribution shows a trend of high at the top and low at the bottom, and the temperature in the domain continues to increase with time.

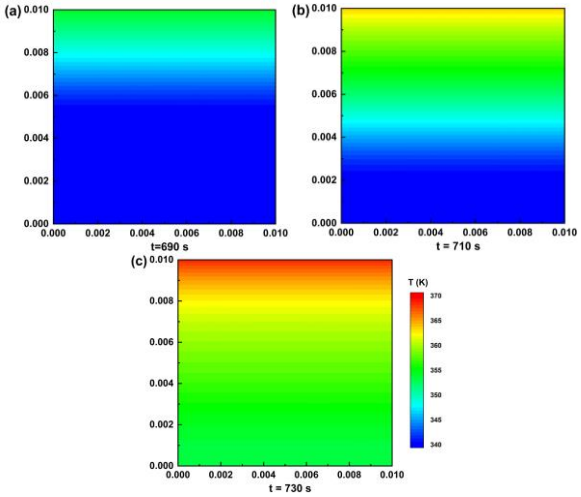

Fig. 5 Temperature distribution at different times

4.1.2 Concentration and conversion degree evolution

The concentration evolution with time is illustrated in Fig. 6. The desorption reaction is observed at point 1 at 665 s. The concentration of the salt hydrate decreases sharply and eventually becomes 0. The reaction duration was short. The faster change in concentration at point 3 is attributed to the rapid reaction caused by rapid heat diffusion in the upper part. Since the domain is closed, the desorption of salt hydrate will lead to increased concentrations of anhydrous salt and water vapor, as depicted in Fig. 6 (b) and (c).

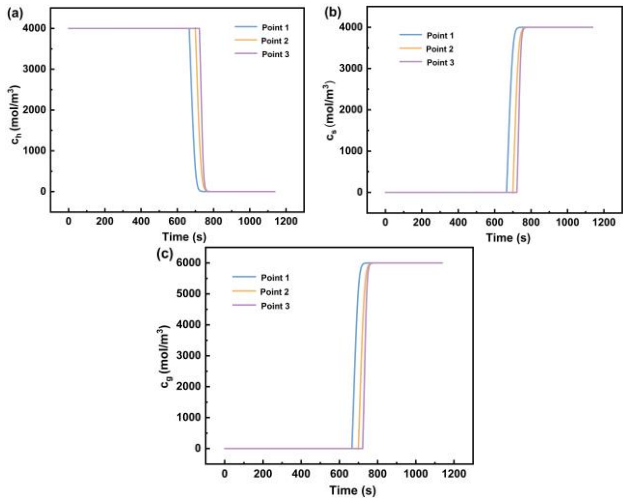

Fig. 6 Evolution of the concentrations of (a) salt hydrate, (b) anhydrous salt and (c) water vapor with time

The variation of material concentration fields with time during thermochemical heat storage process is demonstrated in Fig. 7. The upper part of the material reaches the chemical reaction temperature first, and the salt hydrate is desorbed earlier, resulting in a decrease in concentration. As the temperature in the lower domain increases, the salt hydrate desorbs and transforms into anhydrous salts and water vapor. It is observed that salt hydrate has similar concentration distributions as anhydrous salts and water vapor but exhibits opposite behavior. The variation of conversion degree with time is presented in Fig. 8. The conversion degree is a function of the salt hydrate concentration, so its change trend is similar to that of salt hydrate.

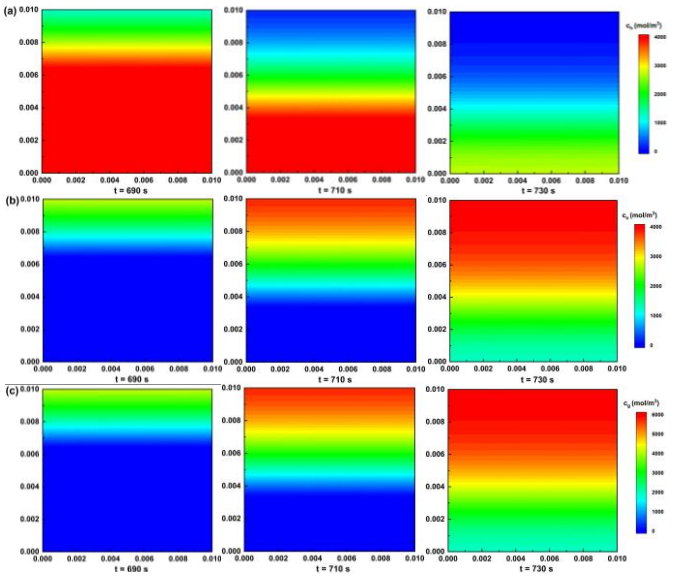

Fig. 7 Concentration distribution of (a) salt hydrate, (b) anhydrous salt and (c) vapor at different times

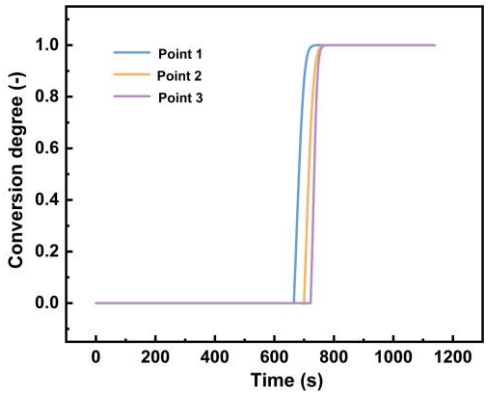

Fig. 8 Conversion degree evolution with time

4.1.3 Porosity evolution

The variation of porosity with time in the porous domain is displayed in Fig. 9. Before the chemical reaction occurs, the porosity is constant. When the chemical reaction temperature is reached, the salt hydrate begins to desorb and the porosity in the porous domain increases as the reaction proceeds. When the chemical reaction is complete, the porosity remains constant. The rapid change in porosity observed at point 3 is attributed to the rapid chemical reaction caused by rapid thermal diffusion in the upper region.

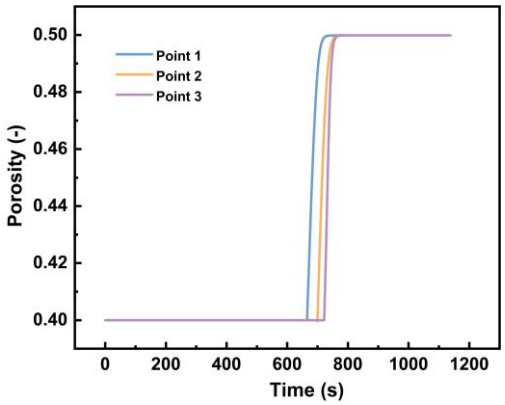

Fig. 9 Porosity evolution with time

Fig. 10 reveals the porosity distribution in the domain during the thermochemical heat storage process. The porosity of the material shows significant inhomogeneity in both time and space, with porosity decreasing from top to bottom. From Eq. (18), the porosity is a function of the conversion degree. Therefore, the porosity shows a similar distribution as the conversion degree.

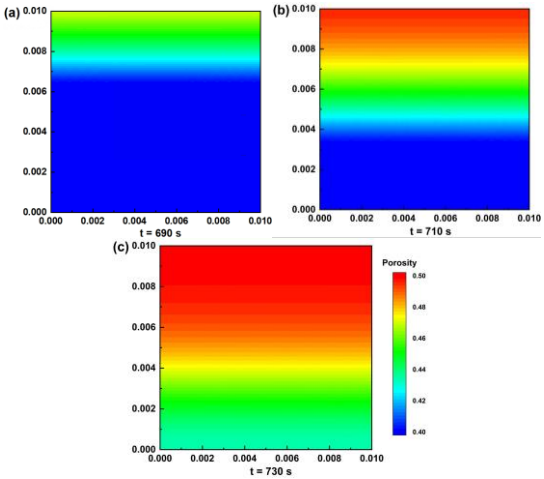

Fig. 10 Porosity distribution at different times

4.2 Parametric analysis

4.2.1 Effect of heat flux

The effect of different heat fluxes on the reaction start-up time is depicted in Fig.11. The increase in heat flux effectively reduces the start-up time. When the heat flux increases from 500 W/m^2 to 2000 W/m^2, the start-up time is shortened from 1432 s to 279 s. Therefore, the heat flux input of the thermochemical energy storage system should be increased as much as possible in the subsequent design.

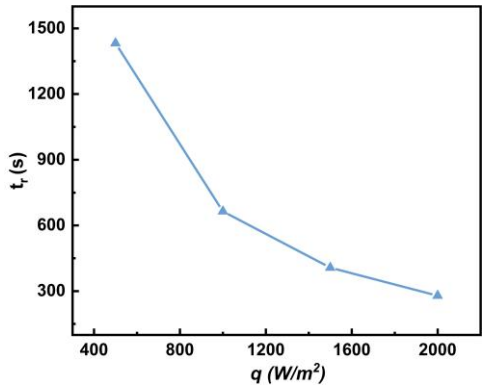

Fig. 11 Reaction initiation time at different heat fluxes

4.2.2 Effect of heat loss

Fig. 12 indicates the reaction start-up time of the thermochemical heat storage system under different heat losses. When there is heat loss in the system, the start-up of the desorption reaction will be delayed, and the reaction start-up time will increase with the rise of heat loss. Therefore, in subsequent designs, the heat loss of the thermochemical heat storage system should be minimized as much as possible, such as increasing the thickness of the system insulation layer to reduce the

reaction start-up time and improve the system efficiency.

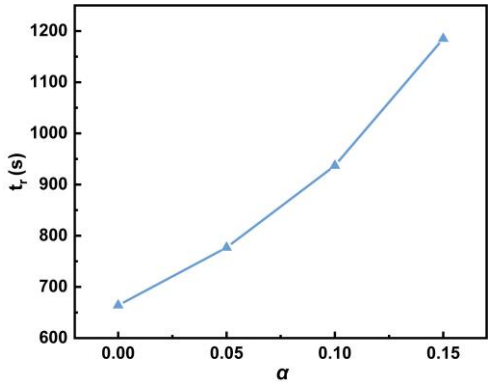

Fig. 12 Reaction initiation time at different heat losses

5. CONCLUSIONS

In this paper, a two-dimensional numerical model of the heat storage process of K_2CO_3 is established considering the change of porosity with conversion degree and the flow of water vapor. The variation and distribution of parameters such as temperature, concentration and porosity during thermal storage are numerically analyzed. The effects of various parameters on system performance are explored. The findings demonstrate that the temperature, concentration and porosity distributions are similar in the porous domain. The porosity of the heat storage material exhibits significant inhomogeneity in both time and space, and it increases continuously as the reaction proceeds. Increasing heat flux and reducing heat loss can effectively reduce the reaction start-up time. Parametric study offers valuable insights for designing and optimizing TCES material and system. For example, by introducing greater heat flux and increasing insulation thickness to enhance system performance.

ACKNOWLEDGEMENT

This work was financially supported by the National Science Fund for Excellent Young Scholars [No. 52022066].

REFERENCE

[1] Olabi AG, Onumaegbu C, Wilberforce T, Ramadan M, Abdelkareem MA, Al–Alami AH. Critical review of energy storage systems. Energy. 2021;214:118987.

[2] Dinker A, Agarwal M, Agarwal G. Heat storage materials, geometry and applications: A review. Journal of the Energy Institute. 2017;90(1):1-11.

[3] Aydin D, Casey SP, Riffat S. The latest advancements on thermochemical heat storage systems. Renewable and Sustainable Energy Reviews. 2015;41:356-67.

[4] Da Y, Xuan Y, Teng L, Zhang K, Liu X, Ding Y. Calcium-based composites for direct solar-thermal conversion and thermochemical energy storage. Chemical Engineering Journal. 2020;382:122815.

[5] Xueling Z, Feifei W, Qi Z, Xudong L, Yanling W, Yeqiang Z, et al. Heat storage performance analysis of ZMS-Porous media/CaCl2/MgSO4 composite thermochemical heat storage materials. Solar Energy Materials and Solar Cells. 2021;230:111246.

[6] Luo X, Li W, Wang Q, Zeng M. Numerical investigation of a thermal energy storage system based on the serpentine tube reactor. Journal of Energy Storage. 2022;56:106071.

[7] Sögütoglu L-C, Steiger M, Houben J, Biemans D, Fischer HR, Donkers P, et al. Understanding the hydration process of salts: the impact of a nucleation barrier. Crystal Growth & Design. 2019;19(4):2279-88.

[8] Mahmoudi A, Donkers PA, Walayat K, Peters B, Shahi M. A thorough investigation of thermochemical heat storage system from particle to bed scale. Chemical Engineering Science. 2021;246:116877.

[9] Shkatulov A, Houben J, Fischer H, Huinink H. Stabilization of K2CO3 in vermiculite for thermochemical energy storage. Renewable Energy. 2020;150:990-1000.

[10] Zhao Q, Lin J, Huang H, Xie Z, Xiao Y. Enhancement of heat and mass transfer of potassium carbonate-based thermochemical materials for thermal energy storage. Journal of Energy Storage. 2022;50:104259.

[11] Kant K, Shukla A, Smeulders DM, Rindt CC. Performance analysis of a K2CO3-based thermochemical energy storage system using a honeycomb structured heat exchanger. Journal of Energy Storage. 2021;38:102563.

[12] Kharbanda JS, Yadav SK, Soni V, Kumar A. Modeling of heat transfer and fluid flow in epsom salt (MgSO4• 7H2O) dissociation for thermochemical energy storage. Journal of Energy Storage. 2020;31:101712.

[13] Chate A, Sharma R, Dutta P. Studies on a potassium carbonate salt hydrate based thermochemical energy storage system. Energy. 2022;258:124873.

[14] Balasubramanian G, Ghommem M, Hajj MR, Wong WP, Tomlin JA, Puri IK. Modeling of thermochemical energy storage by salt hydrates. International Journal of Heat and Mass Transfer. 2010;53(25-26):5700-6.